Electronic Supplementary Material (ESI) for Journal of Materials Chemistry C.

Supporting Information

To improve efficiency of thermally activated delayed fluorescence OLEDs by controlling the horizontal orientation through optimizing stereoscopic and linear structures of indolocarbazole isomers

Songpo Xiang,[a] Xialei Lv,[a] Shuaiqiang Sun,[a] Qing Zhang,[a] Zhi Huang,[a] Runda Guo,[a] Honggang Gu,[b] Shiyuan Liu,[b] Lei Wang*[a]

[a] Wuhan National Laboratory for Optoelectronics, Huazhong University of Science and Technology, Wuhan, 430074, P. R. China

[b] State Key Laboratory of Digital Manufacturing Equipment and Technology, Huazhong University of Science and Technology, Wuhan 430074, China.

*Email: wanglei@mail.hust.edu.cn

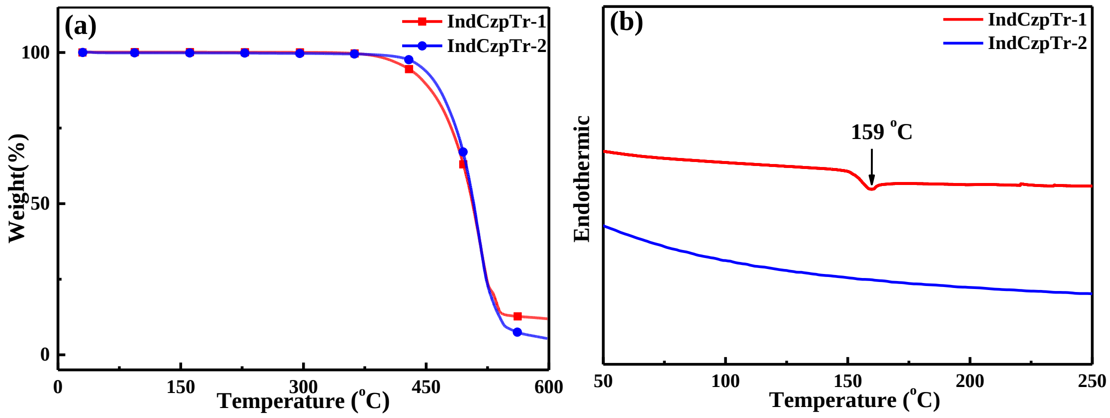

Fig. S1. a) TGA thermograms and b) DSC curves of **IndCzpTr-1** and **IndCzpTr-2**.

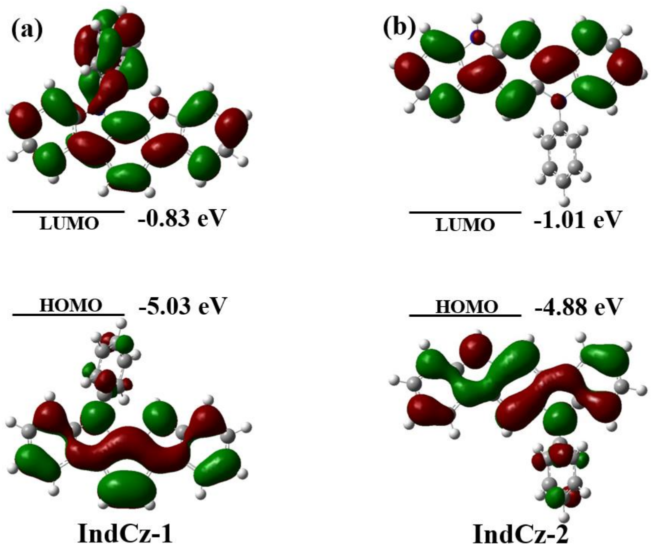

Fig. S2. The HOMO and LUMO distribution of a) **IndCz-1** and b) **IndCz-2**, and the calculated energy levels.

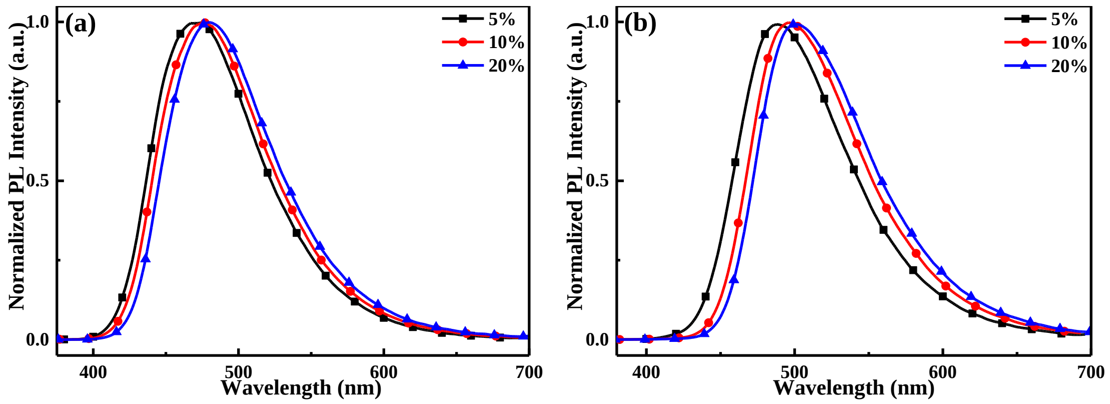

Fig. S3. PL spectra of a) **IndCzpTr-1** and b) **IndCzpTr-2** at different concentrations in doped films.

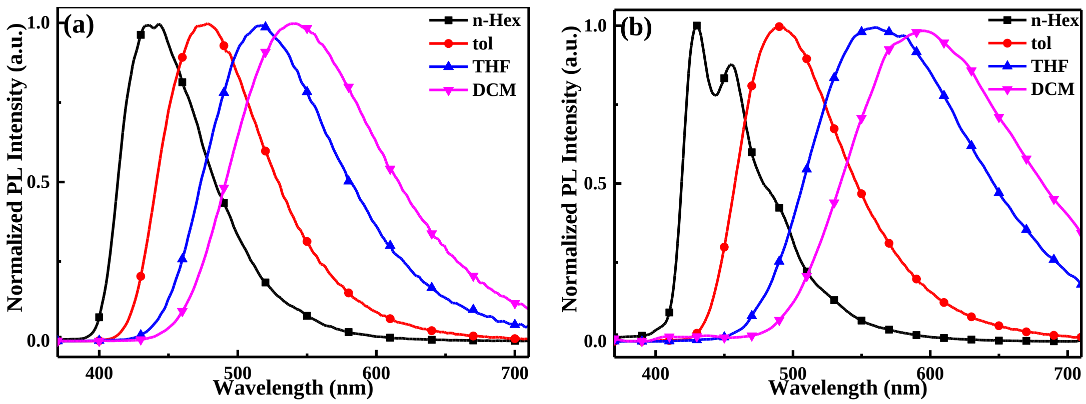

Fig. S4. Solvatochromic of a) **IndCzpTr-1** and b) **IndCzpTr-2** in different solvents.

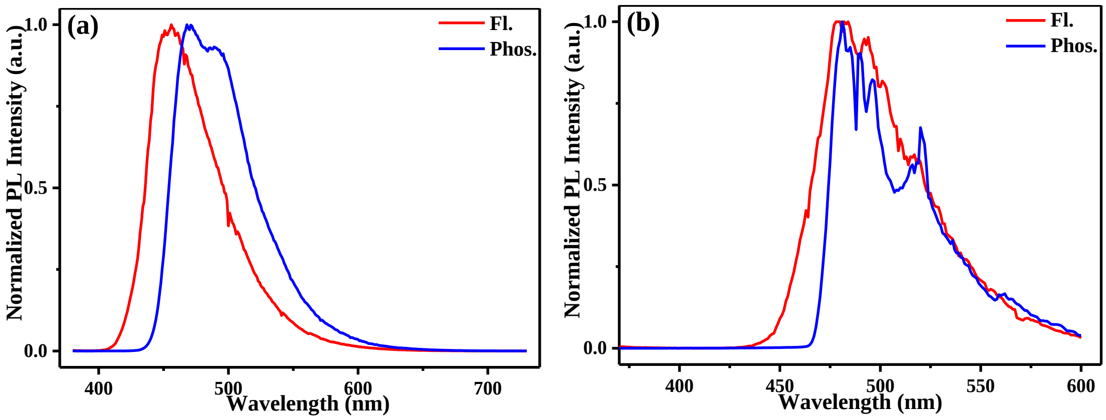

Fig. S5. Low temperature fluorescence and phosphorescence spectra of a) **IndCzpTr-1** and b) **IndCzpTr-2** at 77 K.

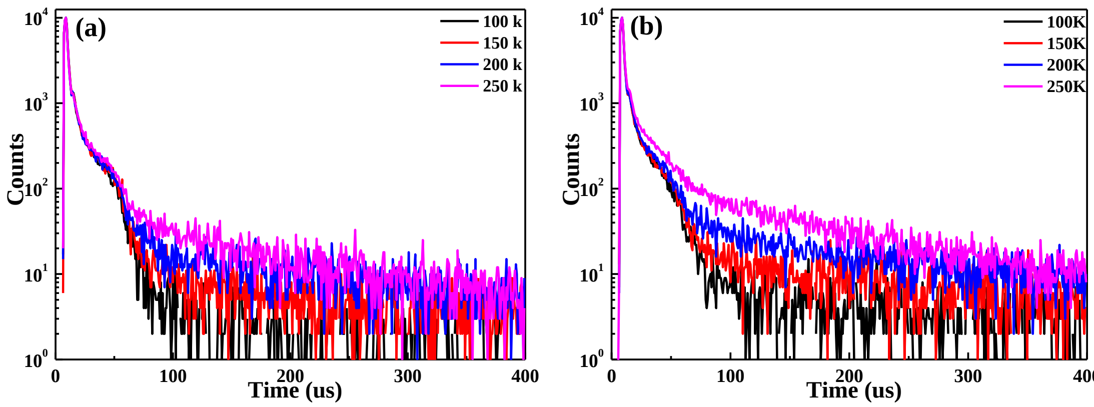

Fig. S6. Temperature-dependence of the transient PL characteristics for a) **IndCzpTr-1** and b) **IndCzpTr-2** in doped films.

Table S1. Optical constants of **IndCzpTr-1** and **IndCzpTr-2**.

Compound	τ_p[a] (ns)	τ_d[a] (μs)	Φ_p[b] (%)	Φ_d[b] (%)	Φ[c] (%)	k_{RISC} ($10^4 s^{-1}$)	k_F ($10^7 s^{-1}$)	k_{ISC} ($10^7 s^{-1}$)	k_{TADF} ($10^4 s^{-1}$)
IndCzpTr-1	11.09	25.48	73.9	4.7	78.6	3.29	6.66	0.54	3.29
IndCzpTr-2	8.83	34.31	66.2	5.7	71.9	2.15	7.50	0.90	2.13

[a] τ_p (the prompt lifetime) and τ_d (the delayed lifetime) were obtained from transient PL decay of doped films. [b] Φ_p (the prompt PLQY) and Φ_d (the delayed PLQY) were estimated according to the prompt and delayed proportions in transient decay curves. [c] Absolute PLQY of doped films measured with integrating sphere.

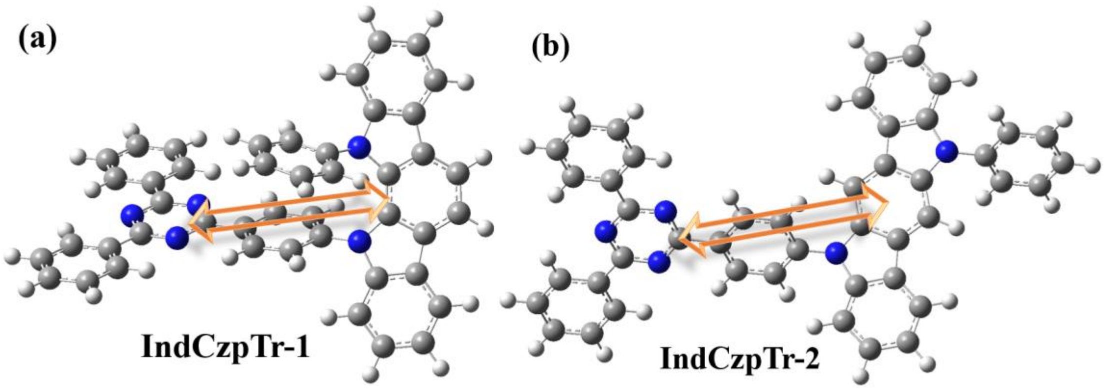

Fig. S7. The direction of the calculated transition dipole moment (as indicated by the colored arrow) of a) **IndCzpTr-1** and b) **IndCzpTr-2**.

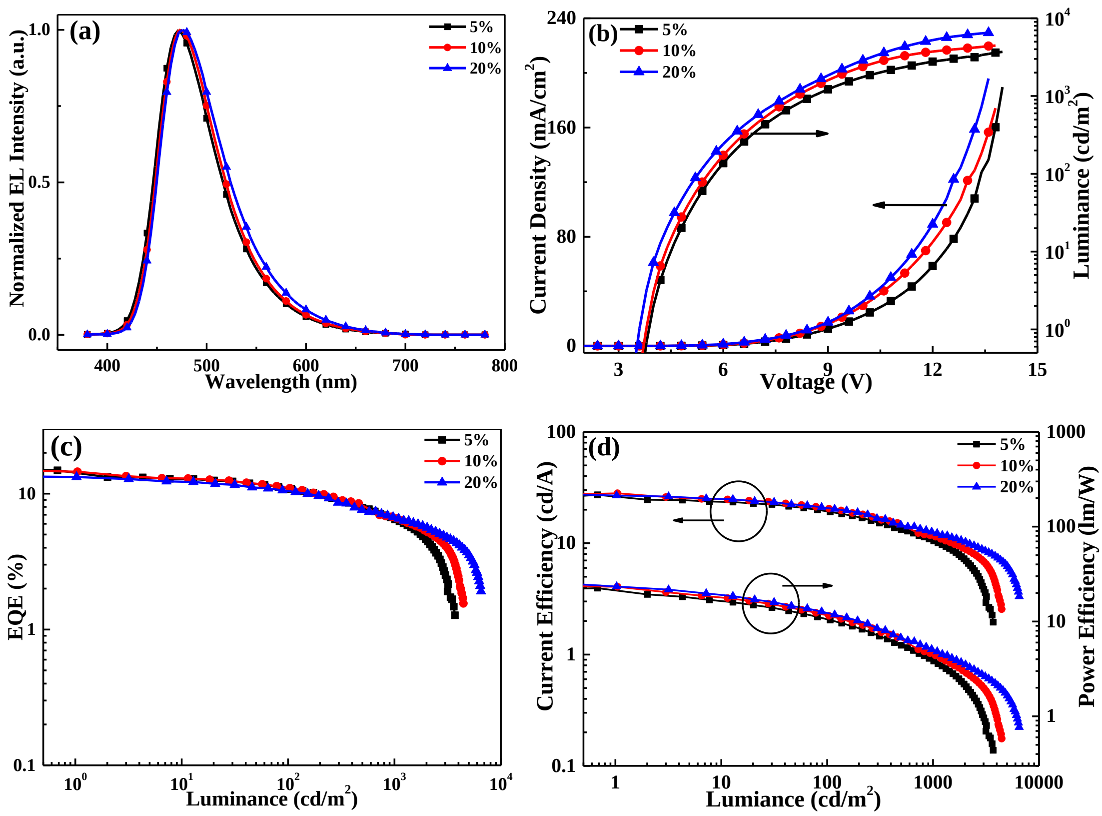

Fig. S8. a) EL spectra at 100 cd/m^2, b) current density–voltage–luminance (J–V–L) characteristics, c) EQE–luminance characteristics, and d) CE–luminance characteristics and PE–luminance characteristics for device of **IndCzpTr-1** with different doped concentrations.

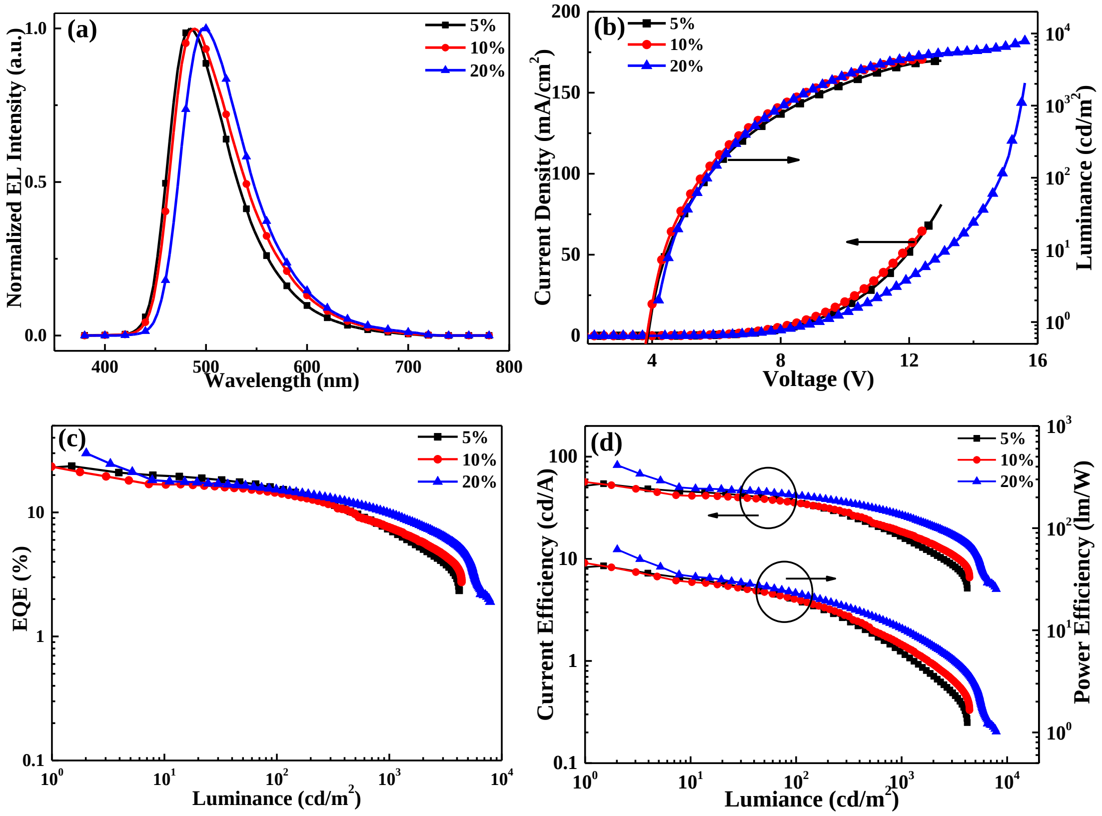

Fig. S9. a) EL spectra at 100 cd/m^2, b) current density–voltage–luminance (J–V–L) characteristics, c) EQE–luminance characteristics, and d) CE–luminance characteristics and PE–luminance characteristics for device of **IndCzpTr-2** with different doped concentrations.

Table S2. EL performance of representative OLEDs with different doped concentrations of **IndCzpTr-1** and **IndCzpTr-2** devices.

EML	concentration	V_{on}^{a} (V)	L_{max}^{b} (cd m^{-2})	EQE_{max}^{c} (%)	CE_{max}^{c} (cd A^{-1})	PE_{max}^{c} (lm W^{-1})	$CIE_{(x,y)}$	λ_{EL}^{d} (nm)
mCBP: IndCzpTr-1	5%	3.9	3701	14.9	27.2	22.4	(0.17,0.25)	472
	10%	3.8	4452	14.5	28.1	23.2	(0.17,0.27)	472
	20%	3.6	6520	13.3	26.8	23.4	(0.18,0.29)	476
mCBP: IndCzpTr-2	5%	3.9	4185	23.6	54.3	42.7	(0.19,0.38)	484
	10%	3.9	4396	24.2	56.7	46.3	(0.21,0.42)	488
	20%	4.0	7876	30.0	82.6	61.8	(0.23,0.50)	496

[a] The maximum luminance. [b] operating voltages for onset. [c] the maximum efficiencies of EQE (%), CE (cd A^{-1}) and PE (lm W^{-1}). [d] EL peak wavelength.

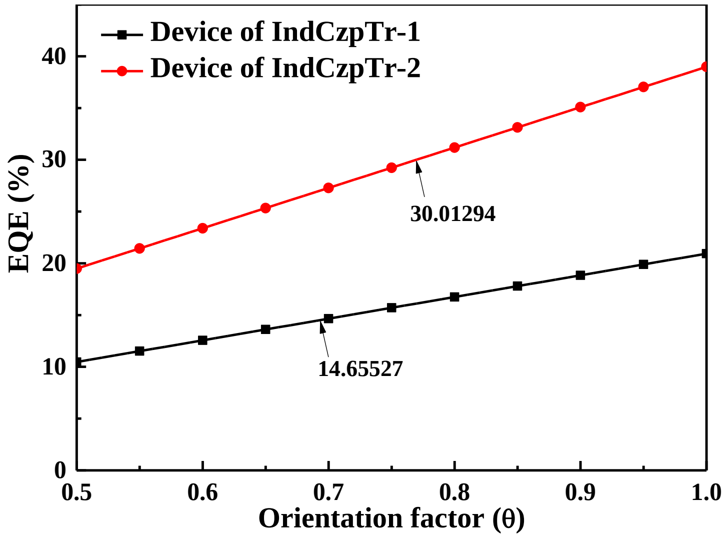

Fig. S10. Calculated results of maximum achievable EQEs as orientation factor.

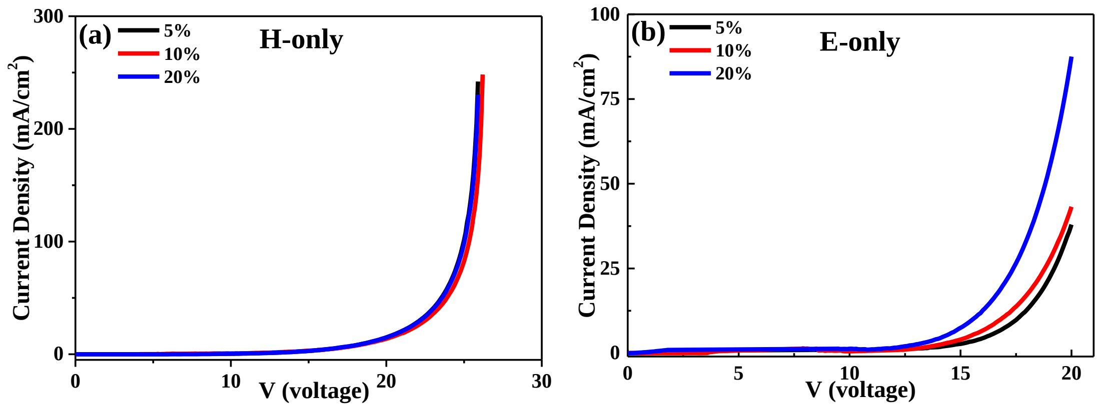

Fig. S11. Current density-voltage characteristics of a) hole-only and b) electron-only devices with different concentrations for **IndCzpTr-1**.

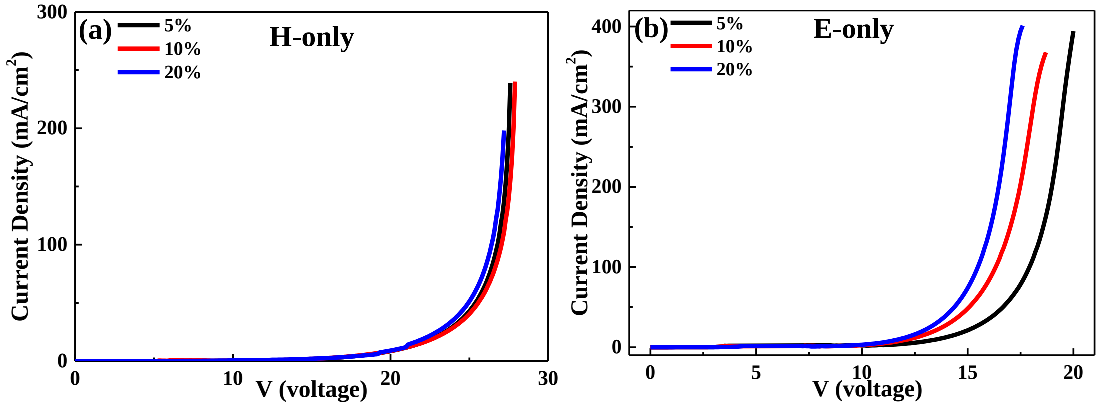

Fig. S12. Current density-voltage characteristics of a) hole-only and b) electron-only devices with different concentrations for **IndCzpTr-2**.